Physicochem. Probl. Miner. Process., 58(5), 2022, 155101

http://www.journalssystem.com/ppmp

Physicochemical Problems of Mineral Processing

ISSN 1643-1049

Introducing key advantages of intensified flotation cells over conventionally used mechanical and column cells

Ahmad Hassanzadeh [1, 2], Mehdi Safari [3], Hamid Khoshdast [4], Mustafa K. Güner [1], Duong H. Hoang [2], Tim Sambrook [5], Przemyslaw B. Kowalczuk [1]

[1] Department of Geoscience and Petroleum, Faculty of Engineering, Norwegian University of Science and Technology, Andersens veg 15a, 7031 Trondheim, Norway

[2] Maelgwyn Mineral Services Ltd, Ty Maelgwyn, 1A Gower Road, Cathays, Cardiff, CF24 4PA, United Kingdom

[3] Minerals Processing Division, Mintek, Private Bag X3015, Randburg 2125, South Africa

[4] Department of Mining Engineering, Higher Education Complex of Zarand, Zarand 7761156391, Iran

[5] Sambrook Metallurgy, 20 Friars Road, Barry Island, Vale of Glamorgan, CF62 5TR, United Kingdom

Corresponding author: ahmad.hassabzadeh@ntnu.no (Ahmad Hassanzadeh)

Abstract: The present paper introduces the key advantages of Imhoflot™, Jameson™, and Reflux™ flotation cells over the conventionally used mechanical and column cells from different perspectives. The impact of slurry mean retention time, bubble size distribution, and energy input was studied for all cell types. The mean retention time in laboratory-scale Imhoflot™ (V030-cell) and Reflux™ flotation cells (RFC100) were measured experimentally using KCl as a tracer. Also, initially a statistical and practical overview of previously installed Imhoflot™, and Jameson™ cells was presented in this work. It was found that more industrial data is available for the Jameson™ cell. The diagnostic results showed that Reflux™, Jameson™, and Imhoflot™ functionally operate similarly based on providing intensive turbulence in the downcomer. They were initially applied to the Australian and the UK coal industries and installed in the cleaning stage of flotation circuits, while there are now more applications in a wide variety of minerals across the world in different flotation stages. First pilot trials on a Russian gold ore were reported operating both Jameson™ and Imhoflot™ cells at the rougher-scalper and cleaner stages providing superior results using the Imhoflot™ cell as rougher-scalper and the Jameson™ at the cleaner. Formation of sub-micron and micron-sized bubbles, effective hydrodynamic characteristics, and low capital and operating costs were reported as major advantages of intensified flotation cells over the conventionally used ones in improving the recoverability of ultra-fine particles. Literature data showed that these cells provide greater gas-hold-up values (40-60%) over the mechanical (5-20%) and column cells (5-25%) with substantially lower power inputs. It was indicated that low mean slurry retention time could lead to a potential enhancement in their throughputs, but further industrial measurements are required to prove this statement. The Reflux™ cell showed a plug-flow mixing regime, while Imhoflot™ V-Cell followed perfect mixing dispersion regime.

Keywords: pneumatic flotation cells, energy input, mean retention time, fine particles, bubble size distribution

1. Introduction

Since mine cut-off grades sharply reduce and ore mineralogies become more complex, ultra-fine grinding appears to be essential in the mineral processing plants (Hassanzadeh et al., 2022). However, as known particle size reduction to fine and ultrafine extents is associated with a high energy consumption leading to several challenges in the entire mining value chain as demonstrated in Fig. 1. The presence of fine and ultrafine particles reduces the grinding efficiency through dramatic changes in the pulp rheology transferring them into the hydrocyclone underflows, which increases the circulating load and lowers the overall feed throughput (Pural et al., 2022). Such fine particles consume a high amount of chemical reagents in flotation processes, and require a longer retention time to be

DOI: 10.37190/ppmp/155101

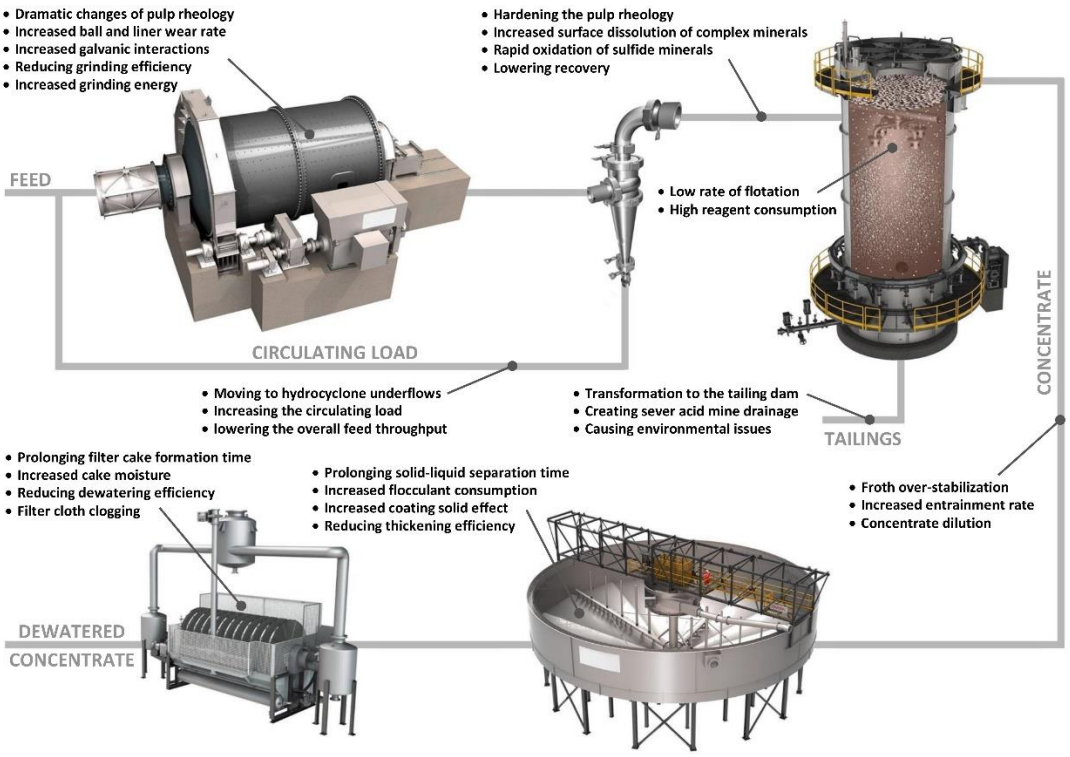

Fig. 1. A schematic image of challenges created by fine and ultrafine particles in a typical concentration plant

recovered (Yianatos et al., 2002; Henríquez et al., 2022). Their low recoverabilities are mainly due to their rapid surface oxidation (Corin et al., 2021), and low particle-bubble capture efficiency (Hassanzadeh et al., 2018; Sajjad and Otsuki, 2022).

In froth flotation circuits, it has been scientifically and technically proven that conventionally used mechanical and column flotation cells are significantly inefficient for recovering fine and ultra-fine particles (Gaudin et al., 1931; Trahar and Waren, 1976; Hassanzadeh et al., 2019). One part of this poor flotation tendency lies in particle properties, including high net particle surface area, rapid surface oxidation, low particle inertial force, and limited particle-bubble collision probability (Gontijo et al., 2007; Safari et al., 2017; Hassanzadeh et al., 2017; Safari et al., 2020a). The other part relates to the cell drawbacks including the inability to produce small bubbles, short retention time for such fine particles, and poor and inefficient turbulence. To overcome these obstacles, researchers either enlarged particle size using flocculation-flotation processes (Yin et al., 2011; Li et al., 2021), applied micro/nano-bubble assisted flotation (Fan et al., 2012; Chipakwe et al., 2021), or utilized intensified cell turbulence (Schubert, 2008; Safari et al., 2014; Testa et al., 2017; Hoseinian et al., 2019). Researchers changed the cell hydrodynamics and invented reactor-separator flotation cells creating remarkable gas hold-up, small bubble sizes, and intensive turbulences (Imhof 2006; Jameson, 2010; Cole et al., 2020). Although they may seem not widely used in the flotation processes, five pneumatic cells were in industrial use in 1928, and this number increased to 11 machines by 1945 (Harbort, 2019). But their application was later limited, while the mechanical flotation cells (MFCs) became a norm in mining and mineral processing industries.

Table 1 lists present incorporations and available technologies in the market for elevating the recoverability of fine particles. Most recently, Hassanzadeh et al. (2022) presented the latest technological developments focusing on some of these cells. A comprehensive historical background of pneumatic flotation cells can be also found elsewhere (Harbort, 2019).

Imhoflot™, Jameson™ and Reflux™ are intensified-flotation cell types operating differently than the older flotation technologies i.e., mechanically agitated and column cells. It should not be forgotten that in the 1930s the Denver™ flotation cell was considered revolutionary, and only in the 1950s using mechanical cells became a norm. A similar story for column cells appears from the early 1960s, however, it was only around the 1980s that a huge interest and demand started. Although pneumatic flotation

Table 1. List of selected companies and corresponded flotation cells available in the market to potentially improve recovery of fine particles

Company	Flotation cell
Metso: Outotec Inc.	Concorde™
Glencore Technology	Jameson™ cell (JFC)
FLSmidth Inc.	Reflux™ flotation cell (RFC)
Eriez	Stack flotation reactor
Maelgwyn Mineral Services Ltd	Imhoflot™ G-cell (IFC)
Allmineral	Allflot™
Woodgrove Technologies	Staged Flotation Reactor (SFR)
MBE Coal & Mineral Technology India PVT. Ltd.*	Pneuflot flotation cell

* There is no more production of these cells in the market

machines e.g., Imhoflot™, and Jameson™ were invented in the 1980s, their application in mining industries compared to mechanical cells has still been limited for some reasons. Detailed information regarding each cell and a historical overview is given elsewhere (Harbort, 2019; Moore, 2021; Mondal et al., 2021; Hassanzadeh et al., 2021). The present work identifies some of the key characteristics of such cells and compares them with the conventional ones. It is known that such pneumatic flotation cells a.k.a. intensified, or reactor-separator type cells possess effective hydrodynamic characteristics, no agitating/moving part, short retention time (Lima et al., 2018), and low capital and operating costs (Hassanzadeh et al., 2022; Safari et al., 2022). For instance, the operating and designing variable of the Jameson™ cell was reported in a series of articles (Cinar et al., 2007; Sahbaz et al., 2013; Ucar et al., 2014).

Currently, over 430 JFCs have been installed in over 30 countries for various operating duties, as summarized in Fig. 2 (Osborn and Eusto, 2015). Table 2 also presents the technical and metallurgical gains of several industrial examples of the Jameson™ flotation cell for various operating circuits reducing the number of mechanically used flotation cells (Moore, 2021). This table has been archived based on information available to the authors. A list of the number of JFCs installed in various operations without giving details of metallurgical achievements was published by Osborn and Eusto (2015). As can be observed, Jameson cells have been extensively applied in the coal beneficiation industry. Generally, it has served as an efficient solution for treating fine coal particles mainly due to the nature of coal and the production of significant amount of fines during the extraction process to the blending step, as well as, during the process of physical separation before the flotation process (Table 2). After the coal industry, optimization of cleaner and recleaner stages had been the next target for JFCs. Although the detailed information about processing circuits examined in Table 2 is not available, there is a fact that an operational aspect of cleaning and re-cleaning circuits is mostly related to a finer feed compared to that at rougher and scavenger stages. Therefore, the effectiveness of JFCs in these duties clearly confirms their ability to handle fine particles. Another interesting point in the application of JFC in rougher circuits is the complete replacement of such circuits including mechanical cells with the JFC. In these conditions, there is no address to the removal of the scavenger circuit in any of the existing reports, which means that the JFCs have been used to specifically treat the fine particles; so that, coarse particles have been next directed to the scavenging circuit, and possibly after a regrinding step, to recover effectively. The use of JFC in solvent extraction processes to remove slimes from pregnant liquors has been also received significant attention (Fig. 2). Fig. 3 demonstrates over 80 installations of Imhoflot™ cells categorized based on the mineral type and country of installations. As seen, these cells were mainly installed for recovering coal/fly ash, copper-molybdenum and potash commissioned predominately in the UK, Chile, and Belarus, respectively. So far, due to the relatively new concept, Reflux™ cells have not been installed. The respective data regarding the Imhoflot™ cells are not available owing to the confidential agreements.

Five flotation cell types are considered in this research study: two conventional i.e., mechanically agitated and column, as well as three intensified flotation vessels i.e., Imhoflot™, Jameson™, and Reflux™. Three fundamental operating properties consisting of i) energy input, ii) slurry mean residence time, and iii) bubble size distributions were conceptually and comparatively studied in detail.

Since there is little information regarding these reactor-separator-type flotation cells, the present work aims at fulfilling this gap in the literature. A conceptual description of such cells was proposed, and the crucial influential factors were analyzed in comparison with the conventionally used mechanical and column flotation cells. This paper is one of the first attempts in compiling recent developments in flotation cell technologies and opens several avenues for their applications.

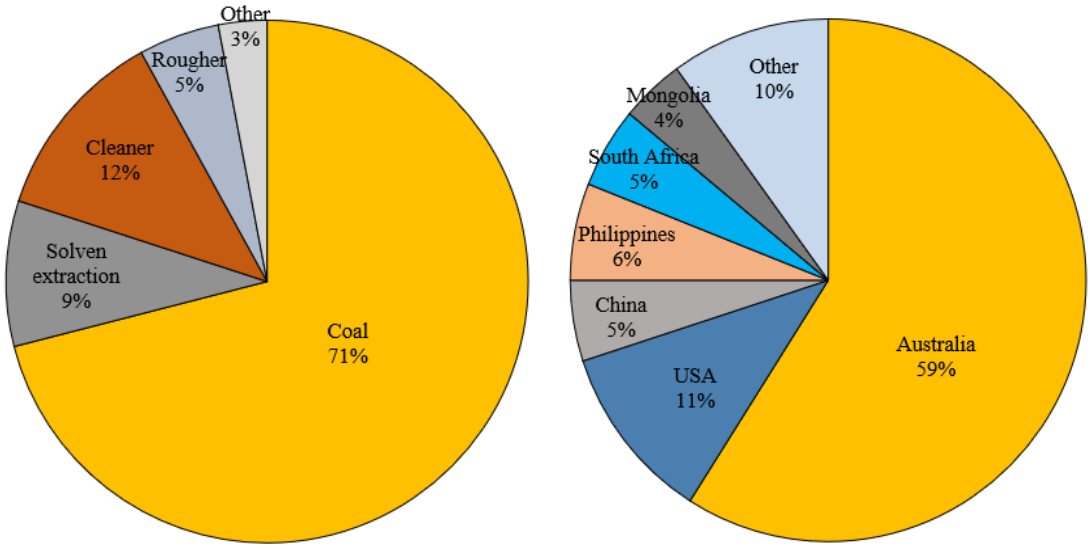

Fig. 2. Jameson™ flotation cell (JFC) installations by (a) application and (b) country (Osborn and Eusto, 2015)

Table 2. Technical and metallurgical achievements of using JFC in coal and mineral beneficiation operations

Concentration plant	Target	No. of JFCs	Placement(P)/Replacement(R)	Improvement results	Reference
Hudbay's New Britannia	Cu	4	As a full-scale flotation line (R)	Removing of 11 MFCs; installation in-progress	Osborn and Eusto, 2015
Ozernoye Zinc Mine	Zn	19	As a full-scale flotation line (R)	Removing of 63 MFCs; >50% footprint reduction	Moore (2021)
Cadia Cu/Au Concentrator Line 1	Cu	3	2 as cleaner/scalper (P) and 1 as recleaner (P)	~6% recovery and ~2.5% garde increase	Akerstorm et al. (2018)
Cadia Cu/Au Concentrator Line 2	Flourine	1	As recleaner (P)	~4.4% garde increase	Akerstorm et al. (2018)
Mount Isa Mines Copper Concentrator Old circuit	Cu	2	As cleaner (P)	Recovery improvevment up to 80%	Lawson et al. (2018)
Mount Isa Mines Copper Concentrator Modified circuit	Cu	2	1 as cleaner/scalper (P) and 1 as recleaner (R)	Reduction from 33 to 5 MFCs; ~5% garde increase	Araya and Lawson (2018)

CSA Mines	Cu	2	1 as cleaner/scalper (P) and 1 as recleaner (R)	Removing of 10 MFCs; ~2% grade increase	Araya and Lawson (2018); Huynh et al. (2014a)
Copper NW Queensland	Cu	1	As cleaner (P)	+1% garde increase	Voigt et al. (2017)
Savannah Nickel Mine	Ni	2	1 as cleaner/scalper (P) and 1 as recleaner (P)	~2% garde increase	Lawson et al. (2017)
Codelco Andina Plant	Cu and Mo	1, PS**	Instead of cleaning circuit with 6 cell columns (R)	No significant improvement in Cu response; ~4 times Mo recovery and ~3 times Mo grade increase	Morin and Lawson (2016)
Glencore's Newlands Mine	Coal fines	2	As full-scale 2-stage flotation line (P)	To achieve a low ash concentrate of 7–12% at up to 70–80% combustible recovery for some feed types with the lower clay content, and 15–17% (ad) ash for coal seams with much higher clay content	Wibberley (2015); Mercuri et al. (2014)
Wesfarmers' Curragh Mine	Coal fines	12	As a full-scale flotation circuit (P)	Treatment of >5 Mt/y	Huynh et al. (2014b)
Barrick's Lumwana operation	Cu	1	As scalper instead of recleaner bank (R)	Removing of 5 MFCs; ~1.3% recovery increase	Araya et al. (2014; 2013)
PanAust's Phu Kham operation	Cu	1	As head cleaner (P)	~0.8% recovery increase	Araya et al. (2013); Bennett et al. (2012)
Clarabelle Mill	Cu	1	Placement in a redesigned flotation circuit (P)	~26% more availability with the same capacity compared to old circuit	Taylor et al. (2012)
Syncrude's Mildred Lake extraction plant	Bitumen	1	As secondary recovery cell (P)	Recovering at least 40% of the non-floating bitumen from tailing stream	Neiman et al. (2012)
Newcrest's Telfer operation	Cu	2	As head cleaner (P)	~10% recovery increase of cleaner circuit	Seaman et al, (2012); (2011)
Xstrata's Cosmos Plant	Ni	1	As head cleaner (P)	Improved pentlandite recoveries, and reduced pyrrhotite recoveries across all size fractions	Curry et al. (2010)

OZ Mineral's Prominent Hill Operation	Cu	1	As head cleaner (P)	Achieving maximum concentrate Cu grade with minimum fluorine levels	Barns et al. (2009)
Red Dog Pb/Zn Mine	Zn and Pb	1	As head cleaner (P)	Zn and Pb absolute recovery gains of 1.0% and 1.5%, respectively	Smith et al. (2008)
Mount Isa lead-zinc concentrator	Pb	1	As head cleaner (P)	~9% Zn grade and ~5% recovery increases	Young et al. (2006)
Zinifex Century Zinc Mine	Zn	1	As prefloat cleaner (P)	~2.5% reduction of Zn recovery to tailings	Pokrajcic et al. (2005)
Hail Creek Coal Preparation Plant	Coal fines	3	As full flotation line (P)	High flotation performance for coal fines	Cowburn et al. (2005)
Goonyella Riverside Mine	Coal fines	6	As full flotation line (R) in single stage operation	Removing of all MFCs; ~7% yield increase	Cowburn et al. (2005)
Mount Isa Copper Concentrator	Cu	1	As preflotation (rougher) unit (P)	Improved Cu grade and recovery	Carr et al. (2003)
Mount Isa Copper Slag Plant	Cu	1	As slag cleaner (R)	Removing of 3 columns; ~8% grade increase	Carr et al. (2003)
Mount Isa Copper Flash Plant	Cu	2	as preflotation (rougher) unit (P)	Improved Cu grade and recovery	Harbort (2002)
Minera Alumbrera Concentrator	Cu	14	Two parallel cleaning lines (All P), each including 4 1st cleaners, 1 recleaner and 2 cleaner scavengers	Cu recoveries in excess of 95%	Harbort et al. (2000)
BHP Billiton Mitsubishi Alliance (BMA)	Coal fines	8	In a 2-stage rougher/scavenger configuration (R)	Removing of the entire 32 MFCs; ~3.5% overall yield increase	Caretta et al. (1997)
Philex Mining Corporation	Cu and Au	30	As cleaner scavenger (R) in 3 parallel lines	Replacing of 17 MFCs and 1 Column in roughing and scavenging (for each line); ~50% energy saving and >90% less residence time and footprint area; 2.6% Cu grade, 3.5% Cu and 2.6% Au recovery increase	Harbort et al. (1997)
Company Confidential	PbS line	1	As full rougher/cleaner line (R) in single stage operation	Replacing of 23 MFCs; improved Pb grade and recovery	Hall and Harrison (1995)

	CaF_2 line	1	As cleaner line (R)	Replacing of 49 MFCs; improved CaF_2 grade and recovery	
Cleveland Potash Ltd.	Sylvite	1	As full rougher/cleaner line (R) in single stage operation	Replacing of 16 MFCs; 76.7% energy saving; ~6% KCl recovery increase	Hall and Harrison (1995); Burns et al. (1994a, b)

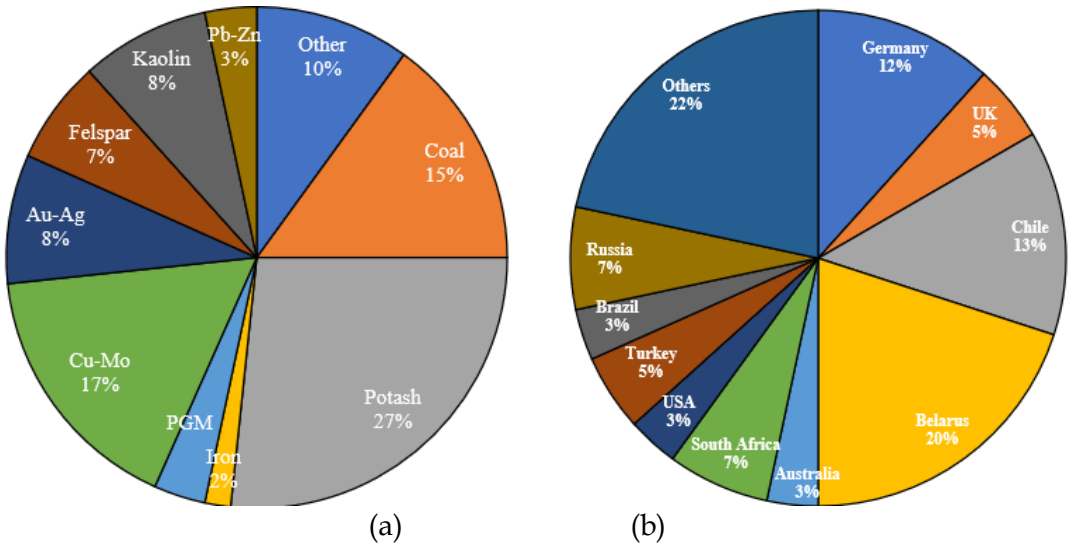

Fig. 3. Installations of Imhoflot™ cells categorized based on a) mineral type, and b) country of destination

2. Materials and methods

2.1. Residence time distribution (RTD) measurements

The slurry retention time determines the number of flotation cells and stages in a circuit required to reach a desirable grade-recovery curve. This term is typically measured by radioactive, pH, and conductivity tracers to monitor slurry/liquid discharge in open- and closed-circuits. A laboratory Imhoflot™ V-030 flotation cell and Reflux™ RFC-100 kit were subjected to the RTD measurements using KCl as a tracer. 30-50 L of water was localized in a conditioning tank before feeding the cell. Circulating water through the tank and cell was stabilized by monitoring feed and tailing pump speeds/flow rates to reach a steady-state condition. Gas flowrate, wash water, bias and other relevant operating parameters were controlled and measured as presented in Table 3. Water properties were measured via the Coupled Plasma Mass Spectrometry (ICP-MS) method and exhibited in Table A1 (supplementary data, Appendix A). Noteworthy, the cell was operated in an open-circuit mode (without re-circulation) in the absence of any reagents. Afterwards, a pre-prepared 30 mL of highly concentrated KCl was instantly injected into the aerator while feeding a specific amount of water flow rate under a desirable aeration rate given in Table 3. A series of time-wised samples were taken from the tailing stream and their conductivity and pH were measured afterward. The obtained data were analyzed through an in-house developed software using N-Mixer and Weller models as described elsewhere (Yianatos et al., 2017; Hassanzadeh, 2017) and calculated by Eq. 1:

$$\tau = \frac{V}{Q} \tag{1}$$

where τ (s) is calculated mean retention time (MRT), V (L) is the effective volume of cell, and Q (L/min) is the water flowrate. Detailed infomation regarding describtion of the effective volume can be found elsewhere (Yianatos et al., 2021).

Weller model represents the mixing conditions by several perfectly mixed reactors in series either with equal or different sizes (Eq. 2):

$$E(t) = \frac{\left(-\frac{t-\tau_{pf}}{\tau_s}-\alpha\right).\exp\left(-\frac{t-\tau_{pf}}{\tau_s}\right)+\alpha.\exp\left(-\frac{t-\tau_{pf}}{\tau_L}\right)}{\tau_L-\tau_s} \quad (2)$$

where $\alpha = \frac{\tau_L}{\tau_L-\tau_s}$, one large perfect mixer (τ_L) and two small perfect mixers in series (τ_s), including a dead time or plug-flow regime (τ_{pf}).

N-Mixer model (Eq. 3) however, contains N-perfect mixer in series along with a plug-flow regime (τ_{pf}).

$$E(t) = \frac{(t-\tau_{pf})^{N-1}\exp\left(\frac{-(t-\tau_{pf})}{\tau}\right)}{\tau^N\Gamma(N)} \quad (3)$$

where N is number of perfect mixers, t is time, τ_{pf} is plug-flow regime, and τ is the MRT of one perfect mixer reactors.

Through normalization process, so-called dimension-less RTD curve (E(θ), Eq. 4), the impact of other variables (e.g., liquid and gas flow rates) were eliminated:

$$E(\theta) = \tau E(t) \quad (4)$$

where $E(t)$ and τ are a dimensional RTD curve and MRT value, respectively. The dimensionless time term (θ) was defined as $\theta = \frac{t}{\tau}$. Further information in this regard can be found elsewhere (Yianatos et al., 2002; Yianatos et al., 2010).

Table 3. Operating parameters of RTD measurements for two studied cells

Flotation cell type	Imhoflot™ flotation cell (IFC)		Reflux™ flotation cell (RFC)	
Property	Flowrate (L/min)	Flux (cm/sec)	Flowrate (L/min)	Flux (cm/sec)
Feed	5.0	0.3	20.0	4.2
Underflow	5.0	0.3	20.0	4.2
Wash water	0.1	0.0	5.0	1.0
Overflow	0.1	0.0	5.0	1.0
Gas	3.0	0.2	10.0	2.1
Bias	0.0	0.0	0.0	0.0
Cell volume (L)	~11		~16	

2.2. Bubble size measurements

A modified McGill bubble viewer was installed for measuring the bubble size distribution in a pilot-scale Imhoflot™ H-16 cell (1.6 m diameter, combined tangential and vertical feed, flowrate 60 m^3/h; self-aspirating aerator) at the feldspar concentration plant in AKW Inc. (Germany), while literature data were used for Jameson™ and Reflux™ flotation cells. To this end, while the Imhoflot™ H-16 cell was operated by processing water, a bubble sampling tube was positioned at a specific location within the separator tank after ensuring the cell works in a steady-state condition. The measurements were performed without any additional collectors and frother because of having residual chemical reagents in the recirculating water. Sampled bubbles were monitored and filmed in the viewing chamber and later analyzed with the image processing toolbox of the MATLAB software (Math works R2021b v9.11, MathWorks, Inc., Natick, MA, USA). The size of approximately 2000-3000 bubbles was measured and statistically analyzed. More detailed information regarding the setup, images processing and bubble size evaluation can be found elsewhere (Hoang et al., 2019a; Hoang et al., 2019b; Hoang et al., 2022).

3. Results and discussions

3.1. Measurement and estimation of mean residence time (MRT)

Fig. 5 exhibits the resultant liquid residence time measurements performed in a laboratory Imhoflot™ and Reflux™ flotation cells and fitted the Weller model. It can be seen that dimention-less RTD curves

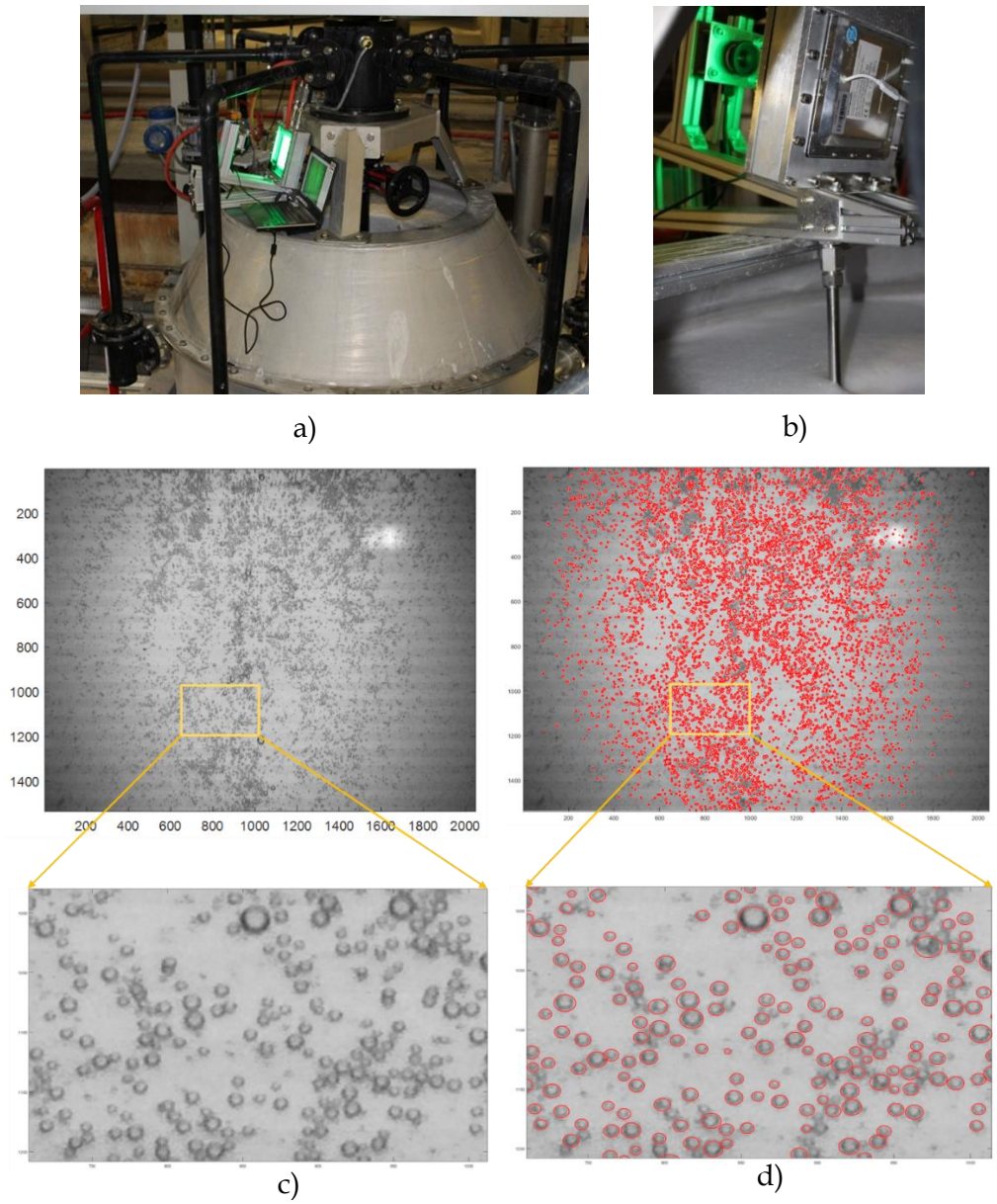

Fig. 4. a) Bubble viewer mounted on the Imhoflot™ H-16 (1.6 m diameter, 60 m^3/h), b) sampling tube, viewing chamber and camera, c) original frame, and d) filtered image with analysed bubbles are marked with a circle

show different patterns for RFC and IFC. The corresponded curve for the RFC represents a very similar distribution to plug flow, while the RTD curve of Imhoflot™ was extended to the right representing typical perfect mixing regime. It was observed that the material remained inside the cell after the mean residence time (MRT). Also, it is important to mention that the cell volumes of RFC and IFC are 16 L and 11 L, respectively, indicating respective feed flow rates of 20 L/min for RFC, which is 4 times faster than Imhoflot™ cell (5 L/min). However, through using dimension-less RTD curves, the impact of volumetric flow rates was eliminated. According to the results presented in Table 4, for both two cells, estimated MRT values by the N-mixer and Weller models were close to the residence time calculated by Eq. 1. In case of RFC, Cole et al., (2021) showed that the liquid residence time in the system ranged between 16–26 s, and the cell residence time was ranged between 23-48 sec. The cell residence time provided was calculated based on the volume of the RFC-100 (~16 L) and all volumetric inlet flows. The active cell volume was the entire cell, and the cell residence time was equal to the cell volume divided by the volumetric feed flow, giving a cell residence time of 25.2 s (Dickinson et al., 2015). Noteworthy, detailed information regarding the RTD measurements, modelling and the impact of other operating parameter will be presented in a separate work in future and only one part of results is presented in this current work.

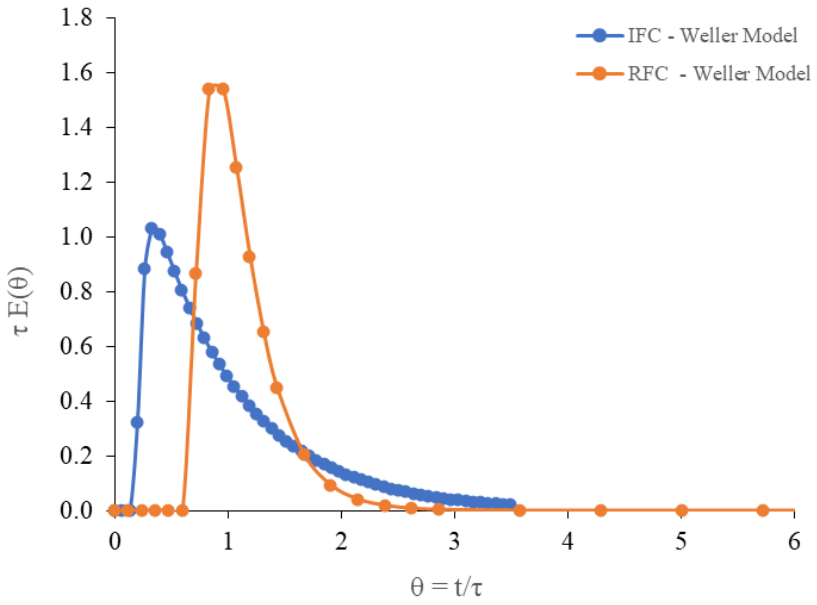

Fig. 5. Presentation of dimension-less RTD data experimentally measured (dots) and modeled (continuous lines) via the Weller model for a V-030 (IFC cell) and RFC-100

Table 4. Calculated and estimated mean residence time (MRT) for Imhoflot™ and Reflux™ cells

Calculated/model	Eq. No.	IFC	RFC
Calculated MRT (sec)	1	144	48
Weller model (sec)	2	157	68
N-Mixer model (sec)	3	144	51

Measuring MRT for the mechanical and column cells in pilot and industrial scales has been broadly reported in the literature. For instance, Yianatos et al. (2015) measured the MRT values for three different plants and reported an effective residence time of 2-7 min for each mechanical cell (100-250 m^3, self-aerated and forced air). Later, Yianatos et al. (2017) measured and modelled the residence time distribution of industrial cells from seven flotation plants. The results showed that the RTD ranged from 9 to 41 min. The large and small tanks in series (LSTS) and two parallel perfect mixers models could reasonably represent the experimental data compared to the axial dispersion and perfect mixer (PM) models. Kennedy (2008) stated that a column cell typically requires approximately twice the residence time of a 4-cell bank of conventional cells and three times the residence time of a batch laboratory flotation cell. It is clear that the conventional cells need long retention times to achieve an acceptable selective separation for fine and ultrafine particles (Ralston et al., 2007; Ran et al., 2019). On the other hand, providing a shorter retention time for such fraction sizes using pneumatic-type cells can induce some advantages. This is a highly critical factor for fine particles due to being oxidized through time rendering physicochemical reactions on the particle surfaces and reducing their hydrophobicities/floatabilities (Pokrajcic et al., 2020). Short residence time allows high throughput and the replacement of few cell numbers instead of several conventional cells. For instance, Harbort et al. (1997) reported the reduction in MRT of a mechanical rougher-scavenger (17.9 min) and cleaner-scavenger (30 min) circuits down to 7.5 min and 2.5 min using Jameson™ cells with identical flotation performances.

3.2. Bubble size distribution (BSD)

Bubble size distribution plays a crucial role in the particle-bubble interaction in flotation processes and significantly impacts the rate and recovery of fine and ultrafine particles (Hassanzadeh et al., 2017). As broadly reported, fine and ultrafine particles require small bubbles (i.e., micro- and sub-micron-sized) to be recovered efficiently (Hassanzadeh et al., 2016; Farrokhpay et al., 2021). Fig. 6 presents an

approximative visualization of bubble ranges typically observed in the given cells. These ranges can vary slightly depending on the operating conditions, frother type and dosages, slurry temperature, particle properties, and mono and multivalent ions in the cell (Vazirizadeh et al., 2016; Safari et al., 2020b). As seen, conventional flotation cells (i.e., MFC and column flotation cell (CFC)) cannot produce bubbles smaller than 0.5 mm with a reasonable concentration due to their natural bubble generation mechanisms (Grau and Heiskanen, 2005; Mazahernasab et al., 2021; Vinnett et al., 2022). Recently, Zahab Nazouri et al. (2021) stated that there is no unique and promising model to be used for predicting the bubble size in a column flotation cell based on the sparger orifice size and other hydrodynamic factors. Further, the Tate Eq. was found inapplicable for the column cells, which was in line with the results of formerly reported study (Hernandez-Aguilar et al., 2006). Following this, Vinnett et al. (2014) analyzed the gas dispersion data of industrial mechanical flotation cells from six Chilean concentrators. They reported a range of 0.5–2.5 cm/s for superficial gas rate, gas holdup (5–25%), bubble size (0.9–4.3 mm), and bubble surface area flux (20–60 $m^2/s/m^2$) (Fig. 6b) which are in line with the results given in Fig. 6a.

In contrast with MFC and CFC, reactor-separator-type cells, where the particle-bubble collision and attachment occur in a downcomer, generate a substantial number of bubbles with a Sauter mean diameter of 0.1-0.7 mm. For example, Fig. 5a demonstrates the BSD of H-16 pilot Imhoflot™ cell manifesting a 0.1-0.4 mm domain for the generated bubbles. The cavitational mechanism created by the venturi tube and specific nuzzle designs generates such micro-bubbles. Almost the same concept is valid for JFC supplying an enormous number of small bubbles with a Sauter mean diameter of 0.2-0.7 mm (Harbort et al., 2000; You et al., 2017). It is worth noting that most of the methods utilized for measuring the BSD have been performed in a two-phase (liquid-gas) system and ex-situ, while an accurate technique applicable in dynamic, in-line, and at a three-phase (liquid-solid-gas) environment is substantially required. A broadly applied approach for measuring BSD is the photographic and optical techniques, while more detailed information regarding different approaches is given elsewhere (Khoshdast et al., 2022). Generally, there is limited practical data in the literature concerning the bubble size distributions performed in such cells, and further experimental data is required.

It is well-known that a pneumatic reactor separator can produce fine bubbles without the need for a conventional rotor-stator system. The Maelgwyn's Imhoflot aerator/reactor is designed based on high shear stress, high turbulence and high acceleration of the flow. There are some mechanisms for the bubble break-up, i.e., i) the Rayleigh-Plateau instability of bubbles in shear flow (Liao and Lucas, 2009), ii) the impact of liquid accelerated flow inertia according to the Kolmogorov-Hinze approach (Drenckhan and Saint-Jalmes, 2015), and iii) Richtmyer-Meshkov instability of bubbles under high acceleration (Chu et al., 2019). Fig. 7 shows a typical bubble distribution obtained from an Imhoflot H-16 cell in a feldspar flotation plant using only process water. The feed flowrate was about 66 m^3/h; the self-aspirated aerator type was used with an air flowrate of 5.7 m^3/h. Note that the bubbles that are created in the aerator might be smaller than the bubbles entering the measuring chamber due to bubble coalescence.

According to the given information in the literature, in the case of RFC, at the highest feed-to-gas flux ratio of 9.1, the bubble diameters were remarkably small, approaching a mean value of 0.37 mm at a feed flux of 15.4 cm/s. These micro-bubbles were observed to be only a small portion of the overall population of bubbles. Hence, the reported diameters were a conservative overestimate of the mean bubble diameters, and the actual mean diameters were found slightly smaller. The bubble surface flux increased to an extraordinary 600 s^{-1}, based on a mean bubble diameter of 0.55 mm, while the underflow liquid flux was 9.5 cm/s and bubble surface flux between 178-600 s^{-1} (Jing et al., 2014). The bubble size at the end of the downcomer for an ion flotation process, and the top size of the bubbles for the lower two j_o/j_g ratios were declared around 0.74 mm (Baynham et al., 2020), where j_o was feed flux (cm/s) and j_g superficial gas velocity (so-called gas flux) (cm/s).

3.3. Energy input

A grade-recovery curve is an explicit demonstration of the inefficiency of conventional flotation cells for recovering both fine and coarse fractions (Lynch et al., 1981). Fig. 8 schematically illustrates the technological developments for raising either tail (via fine flotation systems, FFS) or trunk (by coarse flotation system, CFS) based on either the energy input or energy consumption (Safari et al., 2016b).

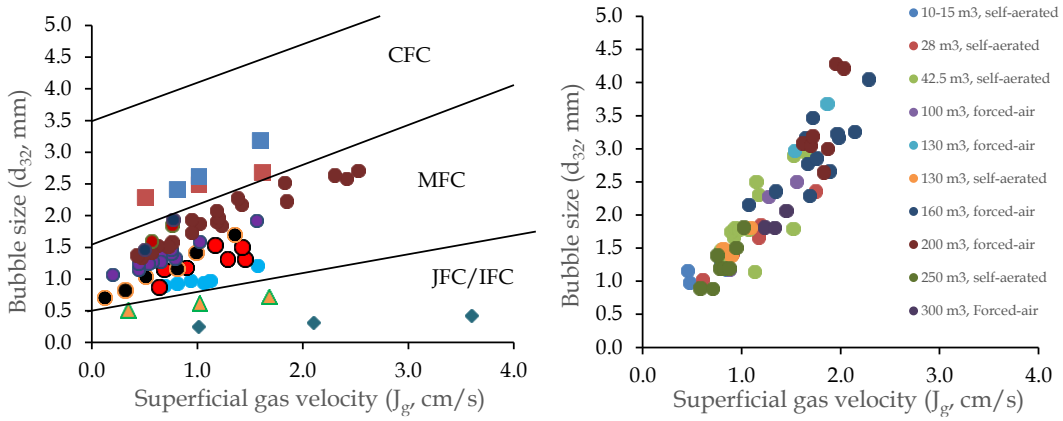

Fig. 6. (a) A demonstrative graph of the bubble size range for five types of flotation cells (circles represent: mechanical flotation cell (MFC), squares: column flotation cell (CFC), triangle: Jameson™ flotation cell (JFC) and diamond: Imhoflot™) (Huynh et al., 2020). There is no information available for the RFC. (b) Example of six Chilean concetration palnts (Vinnett et al., 2014)

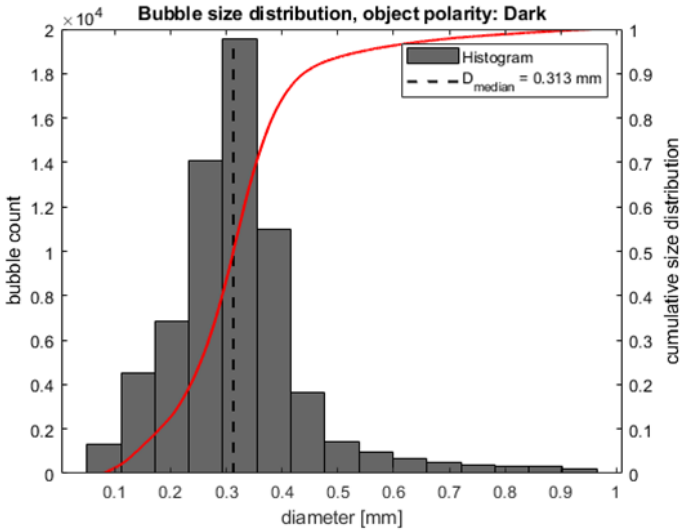

Fig. 7. A typical bubble size distribution generated by an Imhoflot H-16 (d_{median} = 313 µm; d_{mean} = 309 µm and d_{32} = 400 µm)

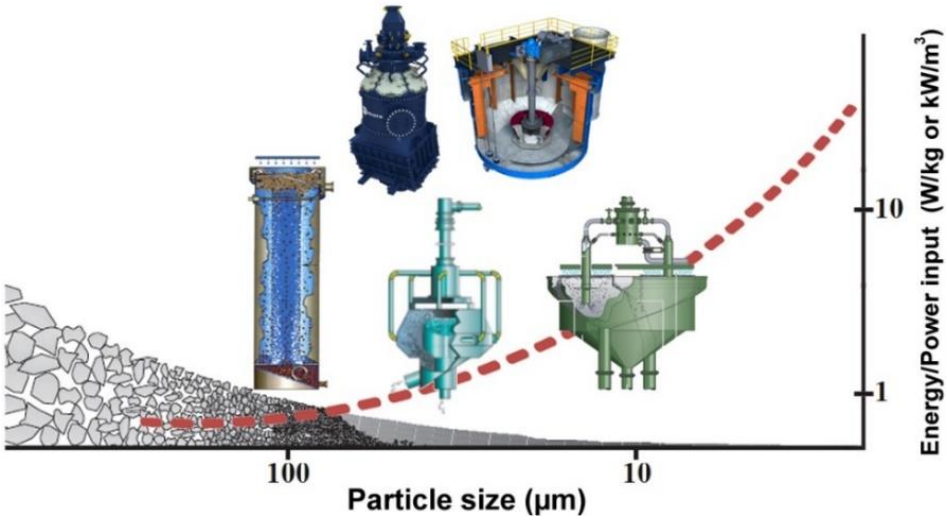

Fig. 8. An overview of existing flotation equipment based on energy consumption and particle size (Hassanzadeh et al., 2021)

It has been widely reported that fine and ultrafine particles require intensive turbulence to reach desirable particle-bubble collision efficiency, which is predominantly controlled by the hydrodynamic properties of the cell (Schubert 2008; Kouachi et al., 2017). The typical energy input used in industrial mechanical cells (a.k.a. tank cells) ranges from 0.6 to 3 kW/m^3 (Deglon et al., 2000; Safari et al. 2016a), although energy levels of up to 12 kW/m^3 are reported for fine particle applications. By enlarging the flotation cell volume, most of the energy is consumed for suspending the slurry than maximizing the particle-bubble interactions (Hoang et al., 2019a). For example, it was shown that cells with a volume of higher than 300 m^3 reduce the specific energy input of 0.5-0.7 kW/m^3, which is 1 kW/m^3 for smaller cells. The summarized energy input data for all studied cells are shown in Table 5. It is worth to note that presented data are an average range of energy input data reported by researchers and flotation cell manufacturers (Hassanzadeh et al., 2022). The average range of energy input data is included all components around the floatation cell including energy requirement for agitation, pumping and air supply. The second important point here is that the energy input unit is kW used per m^3 of the cell volume and not the flowrate going through the flotation cell.

Table 5. Summarized energy input data for all studied cells

Cell type	MFC	CFC	RFC	IFC	JFC
Energy input (kW/m^3)	0.6-5	0.5-2	0.5-3	0.5-1.5	1-7

Mechanical cells have an inherently inhomogeneous distribution of energy input through the cell, with high energy input found near the impeller and much lower levels in the bulk of the cell (Koh and Schwarz, 2003). The fact that the processes of particle suspension, bubble break-up, and energy generation are all interdependent makes it difficult or impossible to optimize the conditions for flotation (Schubert, 2008). Despite these weaknesses, the robustness of the design has meant that mechanical cells overwhelmingly dominate in industrial applications, despite competition from several other cell technologies. There is little quantitative information regarding the energy consumption of reactor-separator flotation cells. Nevertheless, the energy level is lower due to having no moving parts (agitators) and more minor scales compared to the mechanical and column flotation cells.

3.4 . Metallurgical assessments

Fig. 9 demonstrates the first comparison between pilot scale Imhoflot™ and Jameson™ cells operated side-by-side in a Russian gold mine and installed in rougher-scalper (Fig. 9a) and cleaner (Fig. 7b) stages. As can be seen, in rougher-scalper duty, IFC provides more mass pull with a relatively lower enrichment ratio than the JFC, however, the Jameson™ cell shows relatively higher values than the IFC when they were operated as a cleaner. Detailed information regarding the performance of Imhoflot™ G-Cell for another gold ore in Kazakhstanis given elsewhere (Hoang et al., 2022). One reason for such deviation can be

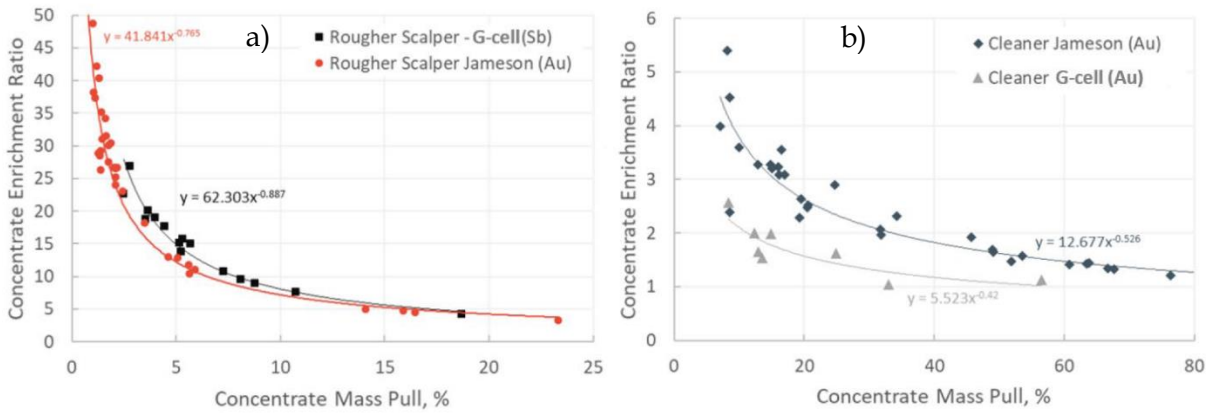

Fig. 9. Concentrate enrichment ratio vs. mass pull using both Imhoflot™ and Jameson™ cells at a) rougher scalper duty and b) cleaner stage (Pyle et al., 2022)

Table 6. A brief comparison between Jameson™ (JFC) and Imhoflot™ (IFC) and Reflux™ (RFC) cells

Property	**JFC**	**IFC**	**RFC**
Wash water as standard	Yes	No	Yes
Froth depth (qualitative)	Medium	Low - Medium	Froth-less system
Froth- pulp interface strength	Low - Medium	Low	n/a
Potential to simplify flotation circuit	Medium	Medium	High
Flexibility of operation for cell dynamics	Low	High	Medium
Level of operations monitoring required	Low	Low	Medium
Level of automation & SCADA integration	Medium	Low	Medium
Level of open-source case studies available on cell performance (2022)	High	Medium	Low
Recirculation load	Medium to high	Low to medium	Low
Speed of flotation kinetics	Medium - Fast	Medium - Fast	Fast
Forced air compressor required	Self-Aspirating	Both options	Forced Air
Bubble size range (mm)	0.300-0.500	0.100-0.300	0.300-0.700
Bubble surface area flux	Medium	Medium	High
Bubble-particle attachment energy	Medium - High	High	Medium- High
Capex per throughput	Medium	Low	Low
Opex per throughput	Low	Low	Low
Plant physical footprint per throughput (m^2)	Medium	Low	Low
Vertical height of installation required	Medium	High	High
Complexity of site installation	Medium	Low	Medium
Maintenance intensity required	Low	Low	Low
OEM or third-party lab testing	OEM	Third-party	OEM and third party
Containerised pilot plant available for deployment to client site	Yes	Yes	Yes
Number of global installations (as of 2022)	431	80	1

the wash water addition on top of JFC, while IFC does not include external wash water. It is also worth noting that the operating conditions and ore properties are unknown and one should include these for future interpretations. Some of the operating and fundamental differences concerning both these cells can be found in Table 6.

Although there are several industrial case studies presenting the metallurgical differences between JFC and CFC and MFC (Huynh et al., 2020), to the best of the author`s knowledge there is not such industrial data reported for RFC at the stage of preparing this manuscript.

4. Conclusions and future works

The present work demonstrates the role of three key parameters of flotation cells (i.e., slurry retention time, bubble size distribution, and energy input,) by categorizing them into two classes i.e., conventional (mechanical and column) and reactor-separator (Imhoflot™, Jameson™, and Reflux™) flotation cells. Some of the parameters were measured experimentally (e.g., RTD of RFC and IFC and BSD of a pilot-scale Imhoflot™) and the rest of data was taken from the literature for analyzing the role of these parameters. The comparative outcomes were summarized from different perspectives. The results showed that JFC, IFC, and RFC are principally operated similarly with slight differences. Their key advantages over the mechanical and column cells were low residence time, high gas hold-up, intensive turbulence in the downcomer, small bubble sizes, low capital and operating costs, small scales, and low maintenance. A pilot scale comparison between Jameson™ and Imhoflot™ flotation cells was reported

indicating their effective operations in a gold concentration plant. A schematic overview of energy consumption using intensified and conventional flotation cells versus particle size was demonstrated showing low energy usage of reactor-separator type cells due to exclusion of impellers from the reactor. The main advantage of Imhoflot™ over Jameson™ and RFC cells was found using no wash water and slightly smallest bubbles.

The following highlights are some of the knowledge gaps and important themes that require further investigations in the future:

- There are serious uncertainties regarding positioning these pneumatic cells in flotation circuits. Additional research works need to be performed to clearly identify their best location within concentration plants supported with fundamental, technical, and metallurgical information.
- There is lack of information regarding predictive modeling and simulation of such cells in software packages. Phenomenological, first-principle, and/or statistically based models are required to be developed for these intensified flotation cells.
- Low level of research data is available on numerical simulation of two-phase (water and gas) or three-phase (solid, liquid, and gas) systems either in aerator or separator parts of such intensified flotation cells.
- There is lack of one-to-one comparison among these cells and even each of them with column or mechanical ones
- Despite existence of industrial proofs-of-concepts for coal in the case of Reflux™ flotation cell, very limited industrial data are available for poly-mineral type ores.
- There is very little information available in terms of the role of recirculation and its optimum value in intensified cells.
- Definition of rougher, scavenger and other stages are unclear for the pneumatic cells and there is a high need for a clarification in this regard.

Acknowledgments

This study was performed and financially supported by The European Union's Horizon 2020 research and innovation program under grant number of 958307 (HARARE project). Authors M.K. Güner and P.B. Kowalczuk thank EIT RawMaterials for the financial support of RFC-Upscaling: New Reflux Flotation Cell Technology Upscaling for Ore Flotation (project number: 20098). We are thankful to Dr. Camilo M. Silva and Mr. Laurentius Tijhuis for analyzing water properties. The authors would like to express their sincere gratitude to Prof. Mehmet S. Celik´s significant scientific contributions to developing our understanding of surface and colloidal chemistries and their application in mineral processing phenomena.

Appendix A

Tap water characteristic was measured through the ICP-MS method during the RTD measurements at the mineral processing pilot plant located in NTNU.

Table A1. Properties of tap water used for the residence time measurements

Component	Mg	S	Ca	Mn	Fe	Co	Ni	Cu	Zn	Sr
Concentration* (ng/mL)	913.49	649.37	21566.67	0.15	110.67	0.07	1.29	14.72	1.32	52.97

* The values are the average of three measurements. The amounts of other trace elements were as Ag< 0.03, Cd< 0.06, Pb< 0.002 U<0.05.

References

AKERSTROM, B., SEPPELT, J., BUBNICH, J., SEAMAN, D., 2018. *Cleaner circuit optimization at Cadia operations*. 14th AusIMM Mill Operators' Conference 2018, Brisbane, Qld., 29–31 August.

ARAYA, R., CORDINGLEY, G., MWANZA, A., HUYNH, L., 2014. *Necessity driving change and improvement to the cleaner circuit at Lumwana copper concentrator*. 46th Canadian Mineral Processors Conference, Ottawa, Ontario, 21–23 January, 329–341.

ARAYA, R., HUYNH, L., YOUNG, M., ARBURO, K., 2013. *Solving challenges in copper cleaning circuits with the Jameson Cell*. 10th International Mineral Processing Conference, Santiago, Chile, 15–18 October, 261–271.

Araya, R., Lawson, V., 2018. The use of the Jameson cell to improve flotation circuit design. Australia.

BARNS, K.E., COLBERT, P.J., MUNRO, P.D., 2009. *Designing the optimal flotation circuit – the Prominent Hill case*. 10th Mill Operators' Conference, Adelaide, South Australia, October 12–14, 173–182.

BAYNHAM, S., IRELAND, P., and GALVIN, K.P. 2020. *Enhancing ion flotation through decoupling the overflow gas and liquid fluxes*, Minerals, 10(12), 1–17. https://doi.org/10.3390/min10121134

BENNETT, D., CRNKOVIC, I., WALKER, P., 2012. *Recent process developments at the Phu Kham copper-gold concentrator*. 11th AusIMM Mill Operators' Conference, Hobart, TAS, 29–31 October, 257–272.

BURNS, M.J., COATES, G., BARNARD, L., 1994a. *Use of Jameson Cell flotation technology at Cleveland Potash Ltd.*, North Yorkshire, England. Trans IMM, Section C 103, C162–167.

BURNS, M.J., COATES, G., BARNARD, L., 1994b. *The use of Jameson Cell flotation technology at Cleveland Potash.* International Fertilizer Association (IFA) Technical Conference, Amman, Jordan, October 2–6, 290–300.

CARETTA, M.F., GRAHAM, J.N., DAWSON, W.J., 1997. *Jameson Cell scale-up experiences at BHP Coal's Goonyella coal preparation plant*, 14th International Coal Preparation Exhibition & Conference, Lexington, Kentucky, 29 April–1 May.

CARR, D., HARBORT, G., LAWSON, V., 2003. *Expansion of the Mount Isa Mines Copper Concentrator phase one cleaner circuit expansion*. 8th Mill Operators' Conference, AUSIMM, Townsville, Queensland, July 22–23.

CHIPAKWE, V., R. JOLSTERÅ, and CHELGANI, S.C., 2021. *Nanobubble-assisted flotation of apatite tailings: Insights on beneficiation options*, ACS Omega, 6, 13888-13894. DOI: 10.1021/acsomega.1c01551

CHU, P., FINCH, J., BOURNIVAL, G., ATA, S., HAMLETT, C. and PUGH, R.J., 2019, A review of bubble break-up. *Advances in colloid and interface science*. 270, 108-122. https://doi.org/10.1016/j.cis.2019.05.010

CINAR, M., SAHBAZ, O., CINAR, F., KELEBEK, S., OTEYAKA, B., 2007. *Effect of Jameson cell operating variables and design characteristics on quartz-dodecylamine flotation system*, Minerals Engineering, 20(15), 1391-1396. https://doi.org/10.1016/j.mineng.2007.09.002

COLE M.J., DICKINSON J.E., GALVIN K.P., 2020. *Recovery and cleaning of fine hydrophobic particles using the Reflux™ Flotation Cell*, Sep. and Purif. Technol. 240, 116641. Doi: 10.1016/j.seppur.2020.116641.

COLE, M. J., GALVIN, K.P., and DICKINSON, J.E. 2021. *Maximizing recovery, grade and throughput in a single stage Reflux Flotation Cell*, Miner. Eng. 163. 106761. https://doi.org/10.1016/j.mineng.2020.106761

CORIN, K.C., MCFADZEAN, B.J., SHACKLETON, N., O'CONNOR, C.T., 2021, Challenges Related to the Processing of Fines in the Recovery of Platinum Group Minerals (PGMs), Minerals 11, 533. https://doi.org/10.3390/min11050533

COWBURN, JA., STONE, R., BOURKE S., HILL, B., 2005. *Design developments of the Jameson Cell*. Centenary of Flotation Symposium, AUSIMM, Brisbane, Australia, June 5–9.

CURRY, D., COOPER, M., RUBENSTEIN, J., YOUNG, M., 2010. *The right tools in the right place: How Xstrata Nickel Australasia increased Ni throughput at its Cosmos Plant.* 42nd Annual Meeting of the Canadian Mineral Processors, Ottawa, Ontario, Canada, January 19–21, 215–234.

DEGLON, D.A., EGYA-MENSAH, D., FRANZIDIS, J.P., 2000. *Review of hydrodynamics and gas dispersion in flotation cells on South African platinum concentrators*, Miner. Eng. 13(3), 235-244. https://doi.org/10.1016/S0892-6875(00)00003-0

DICKINSON, J.E., JIANG, K., and GALVIN, K.P., 2015. *Fast flotation of coal at low pulp density using the Reflux Flotation Cell*, Chem. Eng. Research and Design. 101, 74–81. https://doi.org/10.1016/j.cherd.2015.04.006

DRENCKHAN, W., and SAINT-JALMES, A. 2015. *The science of foaming.* Advances in Colloid and Interface Science, 222, 228-259. https://doi.org/10.1016/j.cis.2015.04.001

FAN, M., ZHAO, Y., and TAO, D., 2012. *Fundamental studies of nanobubble generation and applications in flotation*. Separation Technologies for Minerals, Coal and Earth Resources, 459-469.

FARROKHPAY, S., FILIPPOV, L., FORNASIERO, D., 2021. *Flotation of Fine Particles: A Review*, Miner. Process. and Extract. Metall. Review. 42(7), 473-483. https://doi.org/10.1080/08827508.2020.1793140

GAUDIN, A.M., GROH, J.O. and Henderson, H.B., 1931. *Effect of particle size on flotation*, AIME Technical Publications, 414, 3-23.

GONTIJO, C., FORNASIERO, D., RALSTON, J. 2007. *The limits of fine and coarse particle flotation*, The Canadian Journal of Chemical Engineering, 85, 739-747. https://doi.org/10.1002/cjce.5450850519

GRAU, R.A., HEISKANEN, K., 2005. *Bubble size distribution in laboratory scale flotation cells*, Minerals Engineering, 18(12), 1164-1172. https://doi.org/10.1016/j.mineng.2005.06.011

HALL, S., HARRISON, M., 1995. *New Jameson Cell flotation of industrial minerals*. Industrial Minerals, June, 61–67.

HARBORT, G., *Pneumatic Flotation*, Chapter 7.3. *SME Mineral Processing and Extractive Metallurgy Handbook,* Society for Mining, Metallurgy, and Exploration (SME), 931-957, 2019.

HARBORT, G.J., 2002. *Pilot plant Jameson test work at the Mount Isa Copper Concentrator*. Mount Isa Mine (MIM) Holdings Limited, Internal Report, Australia.

HARBORT, G.J., LAUDER, D., MURPHY, A.S., MIRANDA, J., 2000. *Size by size analysis of operating characteristics of Jameson Cell cleaners at the Bajo de Alumbrera Copper/Gold Concentrator*. 7th Mill Operators Conference, AUSIMM, Kalgoorlie, WA, October 12–14.

HARBORT, G.J., MANLAPIG, E.V., DEBONO, S.K., 2002, *Particle collection within the Jameson cell downcomer*, Miner. Process. and Extrac. Metall. 111(1), 1-10. https://doi.org/10.1179/mpm.2002.111.1.1

HARBORT, G.J., MURPHY, A.S., BUDOD, A., 1997. *Jameson Cell developments at Philex Mining Corporation*. 6th Mill Operators' Conference, AUSIMM, Madang, Papua New Guinea, 6–8 October.

HASSANZADEH, A., 2017. *Measurement and modeling of residence time distribution of overflow ball mill in continuous closed circuit*, Geosys. Eng. 20(5), 251-260. https://doi.org/10.1080/12269328.2016.1275824

HASSANZADEH, A., AZIZI, A., KOUACHI, S., KARIMI, M., CELIK, M.S., 2019. *Estimation of flotation rate constant and particle-bubble interactions considering key hydrodynamic parameters and their interrelations*, Miner. Eng., 141, 105836. https://doi.org/10.1016/j.mineng.2019.105836

HASSANZADEH, A., FIROUZI, M., ALBIJANIC, B., CELIK, M.S., 2018, *A review on determination of particle–bubble encounter using analytical, experimental and numerical methods*, Minerals Engineering, 122, 296-311. https://doi.org/10.1016/j.mineng.2018.04.014

HASSANZADEH, A., KOUACHI, S., HASANZADEH, M., CELIK, M.S. 2017, *A new insight to the role of bubble properties on inertial effect in particle–bubble interaction*, Journal of Dispersion Science and Technology, 38(7), 953-960. https://doi.org/10.1080/01932691.2016.1216437

HASSANZADEH, A., SAFARI, M., HOANG, D.H., 2021. *Fine, coarse and fine-coarse particle flotation in mineral processing with a particular focus on the technological assessments*, In Proceedings of the 2nd International Conference on Mineral Science, Online, 1–15 March 2021. https://doi.org/10.3390/iecms2021-09383

HASSANZADEH, A., SAFARI, M., HOANG, D.H., KHOSHDAST, H., ALBIJANIC, B., KOWALCZUK, P.B., 2022. *Technological assessments on recent developments in fine and coarse particle flotation systems*, Miner. Eng., 180, 107509. https://doi.org/10.1016/j.mineng.2022.107509

HASSANZADEH, A., VAZIRI HASSAS, B., KOUACHI, S., BRABCOVA, Z., ÇELIK, M.S., 2016. *Effect of bubble size and velocity on collision efficiency in chalcopyrite flotation*, Colloids. and Colloids. Surf. A Physicochem. Eng. Asp. 498, 258-267. https://doi.org/10.1016/j.colsurfa.2016.03.035

HENRÍQUEZ, F., MALDONADO, L., YIANATOS, J., VALLEJOS, P., DÍAZ, F., VINNETT, L., 2022, *The Use of Radioactive Tracers to detect and correct feed flowrate imbalances in parallel flotation banks,* Journal, 5, 287–297. https://doi.org/10.3390/j5020020

HERNANDEZ-AGUILAR, J.R., CUNNINGHAM, R., and FINCH, J.A. 2006. *A test of the Tate Eq. to predict bubble size at an orifice in the presence of frother*, Inter. J. of Miner. Process. 79(2), 89–97. https://doi.org/10.1016/j.minpro.2005.12.003

HOANG, D. H., HEITKAM, S., KUPKA, N., HASSANZADEH, A., PEUKER, U.A., RUDOLPH, M., 2019b, *Froth properties and entrainment in lab-scale flotation: A case of carbonaceous sedimentary phosphate ore*. Chemical Engineering Research and Design, 142, 100-110. https://doi.org/10.1016/j.cherd.2018.11.036

HOANG, D.H., HASSANZADEH, A., PEUKER, U.A., RUDOLPH, M., 2019. *Impact of flotation hydrodynamics on the optimization of fine-grained carbonaceous sedimentary apatite ore beneficiation*, Powd. Tech. 345, 223-233. https://doi.org/10.1016/j.powtec.2019.01.014

HOANG, D.H., IMHOF, R., SAMBROOK, T., BAKULIN, A.E., MURZABEKOV, K.M., ABUBAKIROV, B.A., BAYGUNAKOVA, R.K., RUDOLPH, M., 2022. *Recovery of fine gold loss to tailings using advanced reactor pneumatic flotation Imhoflot™*, Miner. Engin. 184, 107649. https://doi.org/10.1016/j.mineng.2022.107649

HOSEINIAN, F.S., REZAI, B., KOWSARI, E., SAFARI, M., 2019. *Effect of impeller speed on the Ni(II) ion flotation*, Geosystem. Eng. 22(3), 161-168. https://doi.org/10.1080/12269328.2018.1520651

HUYNH, L., ARAYA, R., SEAMON, D., MUNRO, P., 2014a. *Improved cleaner circuit design for better performance using the Jameson Cell*. 12th AusIMM Mill Operators' Conference 2014, Townsville, QLD, 1–3 September.

HUYNH, L., KOHLI, I., OSBORNE, D., DE WAAL, H., WALSTRA, C., 2020. *Design and performance aspects of coal flotation –experiences with the Jameson cell*. Jameson Cell-2020 compendium of Technical Papers, 185–196.

HUYNH, L., KOHLI, I., OSBORNE, D.G., 2014b. *Busting the myths of flotation in the Australian coal industry*. Glencore Technology, Australia.

IMHOF, R. US Patent No. 7,108,136 B2, *Pneumatic Flotation Separation Device*, application filed 19. March 2001; published 19. Sept. 2006.

Jameson, G.J., *New directions in flotation machine design*, 2010. Miner. Eng. 23, 11–13, 835-841. https://doi.org/10.1016/j.mineng.2010.04.001

JING, K., DICKINSON, J. E., and GALVIN, K.P. 2014, *Maximizing bubble segregation at high liquid fluxes*. Advanc. Powd. Techn. 25(4), 1205-1211. https://doi.org/10.1016/j.apt.2014.06.003

KENNEDY, D.L., 2008. *Redesign of industrial column flotation circuits based on a simple residence time distribution model*, MSC Thesis, Mining and Minerals Engineering, Virginia Polytechnic Institute and State University, U.S.A.

KHOSHDAST, H., HASSANZADEH, A., KOWALCUK, P.B., FARROKHPAY, S., 2022. *Characterization techniques of flotation frothers - A review*, Miner. Process. and Extrac. Metall. Review. https://doi.org/10.1080/08827508.2021.2024822

KOH, P.T.L., SCHWARZ, M.P., 2003, *CFD modelling of bubble–particle collision rates and efficiencies in a flotation cell*, Miner. Eng. 16, 1055–1059. https://doi.org/10.1016/j.mineng.2003.05.005

KOUACHI, S., VAZIRI HASSAS, B., HASSANZADEH, A., ÇELIK, M.S., BOUHENGUEL, M., 2017. *Effect of negative inertial forces on bubble-particle collision via implementation of Schulze collision efficiency in general flotation rate constant Eq.*, Colloids. Surf. A Physicochem. Eng. Asp. 517, 20, 72-83. https://doi.org/10.1016/j.colsurfa.2017.01.002

LAWSON, V., ANDERSON, G., STRONG, T., 2017. *Improving concentrate grade through smart design and piloting*. 49th Annual Canadian Mineral Processors Operators Conference, Ottawa, Ontario, 17-19 January.

LAWSON, V., DEWAAL, H., HEFEREN, G., ASLIN, N., VOIGT, P., HOURN, M., 2018. *Mount Isa Mines necessity driving innovation*. 50th Annual Canadian Mineral Processors Conference, Ottawa, Ontario, 23–25 January.

LI, M., XIANG, Y., CHEN, T., GAO, X., LIU, Q., 2021. *Separation of ultra-fine hematite and quartz particles using asynchronous flocculation flotation*, Miner. Eng. 164, 106817. https://doi.org/10.1016/j.mineng.2021.106817

LIAO, Y., and LUCAS, D., 2009, *A literature review of theoretical models for drop and bubble breakup in turbulent dispersions*. Chemical Engineering Science, 64, 3389-3406. https://doi.org/10.1016/j.ces.2009.04.026

LIMA, P.N., PERES, A.E.C., GONCALVES, T.A.R., 2018, *Comparative evaluation between mechanical and pneumatic cells for quartz flotation in the iron ore industry*, REM, Int. Eng. J. Ouro Pereto 71(3), 437-442. https://doi.org/10.1590/0370-44672016710179

LYNCH, A.J., JOHNSON, N.W., MANLAPIG, E.V., THORNE, C.G., 1981. *Mineral and Coal Flotation Circuits – Their Simulation and Control, Developments in Mineral Processing Series*, Elsevier Scientific Publishing Company, New York, NY.

MAZAHERNASAB, R., AHAMADI, R., RAVANASA, E., 2021, *Direct bubble size measurement in a mechanical flotation cell by image analysis and laser diffraction technique - A comparative study*, International Journal of Chemical Engineering, 40(5), 1653-1664.

MERCURI, F., OSBORNE, D.G., YOUNG, M.F., 2014. *The future of thermal coal flotation*. 15th Australian Coal Preparation Conference and Exhibition, Broadbeach, Queensland, September.

MONDAL, S., ACHARJEE, A., MANDAL, U., SAHA, B., 2021, *Froth flotation process and its application*, Vietnam Journal of Chemistry, 2021, 59(4), 417-425. DOI: 10.1002/vjch.202100010

MOORE, P., *Flotation factors*, 2021. International Mining Magazine, 36.

MORIN, E., LAWSON, V., 2016. *Jameson Cell project evaluation in the cleaner circuit at Codelco Andina*. 12th International Mineral Processing Conference (Procemin 2016), Santiago, Chile, 26–28 October.

NEIMAN, O., HILSCHER, B., SIY, R., 2012. *Secondary recovery of bitumen using Jameson downcomers*. 44th Annual Canadian Mineral Processors Operators Conference, Ottawa, Ontario, 17-19 January, 115–124.

OSBORNE, D., EUSTON, J., 2015. *Value of the Jameson Cell to the Australian Economy*. Independent Report, MANFORD PTY LTD Coal Technology Consultant, Australia.

POKRAJCIC, Z., HARBORT, G.J., LAWSON, L., REEMEYER, L., 2005. *Applications of the Jameson Cell at the head of base metal flotation circuits*. Centenary of Flotation Symposium, AUSIMM, Brisbane, Australia, June 5–9.

POKRAJCIC, Z., HARBORT, G.J., LAWSON, V., REEMEYER, L., 2020, *Benefits of high intensity flotation at the head of base metal flotation circuits*, Jameson Cell-2020 compendium of Technical Papers, 378-387.

PURAL, Y.E., ÇELIK, M., ÖZER, M., BOYLU, F., *Effective circulating load ratio in mill circuit for milling capacity and further flotation process-lab scale study*, Physicochem. Probl. Miner. Process., 58(5), 2022. 149916. https://doi.org/10.37190/ppmp/149916

PYLE, L., TABOSA, E., VIANNA, S., SINCLAIR, S., VALERY, W., 2022, *Future (and present) trends in circuit design*, IMPC Asia-Pacific 2022, Melbourne 22-24 August, Australia, 1068-1083.

RALSTON, J., FORNASIERO, D., GRANO, S., DUAN, J., AKROYD, T., 2007, *Reducing uncertainty in mineral flotation – flotation rate constant prediction for particles in an operating plant ore*, International Journal of Mineral Processing, 84, 89–98. https://doi.org/10.1016/j.minpro.2006.08.010

RAN, J.C., QIU, X.Y., HU, Z., LIU, Q.J., SONG, B.X., YAO, Y.Q., 2019, *Effects of particle size on flotation performance in the separation of copper, gold and lead*, Powder Technology, 344, 654-664. https://doi.org/10.1016/j.powtec.2018.12.045

SAFARI, M., DEGLON, D., 2020a. *Evaluation of an attachment–detachment kinetic model for flotation*. Minerals 10(11), 1–12. https://doi.org/10.3390/min10110978

SAFARI, M., HARRIS, M., DEGLON, D., 2014. *The effect of energy input on the flotation kinetics of galena in an oscillating grid flotation cell*. In: Proceedings of XXVII International Mineral Processing Congress, Santiago.

SAFARI, M., HARRIS, M., DEGLON, D., 2016b. *The effect of energy input on the flotation of a platinum ore in a pilot-scale oscillating grid flotation cell*. In: Proceedings of XXVIII International Mineral Processing Congress, Quebec, 27–39.

SAFARI, M., HARRIS, M., DEGLON, D., 2017. *The effect of energy input on the flotation of a platinum ore in a pilot-scale oscillating grid flotation cell*, Miner. Eng. 110, 69-74. https://doi.org/10.1016/j.mineng.2017.04.012

SAFARI, M., HARRIS, M., DEGLON, D., LEAL FILHO, L., TESTA, F., 2016a. *The effect of energy input on flotation kinetics*. Inter. J. of Miner. Process. 156, 108-115. https://doi.org/10.1016/j.minpro.2016.05.008

SAFARI, M., HOSEINIAN, F.S., DEGLON, D., LEAL FILHO, L.S., SOUZA PINTO, T.C., 2020b. *Investigation of the reverse flotation of iron ore in three different flotation cells: Mechanical, oscillating grid and pneumatic*, Miner. Eng. 150, 106283. https://doi.org/10.1016/j.mineng.2020.106283

SAFARI, M., HOSEINIAN, F.S., DEGLON, D., LEAL FILHO, L.S., SOUZA PINTO, T.C., 2022. *Impact of flotation operational parameters on the optimization of fine and coarse Itabirite iron ore beneficiation*, Powder Technology 408, 117772. https://doi.org/10.1016/j.powtec.2022.117772

SAHBAZ, O., UCAR, A., OTEYAKA, B., 2013. *Velocity gradient and maximum floatable particle size in the Jameson cell*, Minerals Engineering, 41, 79-85. https://doi.org/10.1016/j.mineng.2012.08.004

SAJJAD, M., and OTSUKI, A., *Correlation between flotation and rheology of fine particle suspensions*, 2022. Metals, 12, 270. https://doi.org/10.3390/met12020270

SCHUBERT, H.J., 2008. *On the optimization of hydrodynamics in fine particle flotation*. Miner. Eng. 21 (12–14), 930–936. https://doi.org/10.1016/j.mineng.2008.02.012

SEAMAN, D.R., BURNS, F., ADAMSON, B., SEAMAN, B.A., MANTON, P., 2012. Telfer processing plant upgrade – the implementation of additional cleaning capacity and the regrinding of copper and pyrite concentrates. 11th AusIMM Mill Operators' Conference, Hobart, TAS, 29–31 October, 373–381.

SMITH, T., LIN, D., LACOUTURE, B., ANDERSON, G., 2008. *Removal of organic carbon with a Jameson Cell at Red Dog Mine*. 40th Annual Meeting of the Canadian Mineral Processors, Ottawa, Ontario, Canada, January 22–24, 333–346.

TAYLOR, A., LAWSON, V., BARRETTE, R., 2012. *Responding to the challenge – necessity driving circuit change*. 11th Mill Operators' Conference, Hobart, TAS, 29 - 31 October.

TESTA, F., SAFARI, M., DEGLON, D., FILHO, L.L., 2017. *Influence of agitation intensity on flotation rate of apatite particles*, REM – Inter. Eng. J. R. Esc. Minas, 70(4), 491-495. https://doi.org/10.1590/0370-44672017700010

TRAHAR, W.J., WARREN, L.J., 1976. *The flotability of very fine particles–a review*. Int. J. Miner. Process. 3(2), 103–131. https://doi.org/10.1016/0301-7516(76)90029-6

UCAR, A., SAHBAZ, O., KERENCILER, S., OTEYAKA, B., 2014. Recycling of colemanite tailings using the Jameson flotation technology, Physicochemical Problems of Mineral Processing, 50(2), 645−655. http://dx.doi.org/10.5277/ppmp140218

VAZIRIZADEH, A., BOUCHARD, J., CHEN, Y., 2016. *Effect of particles on bubble size distribution and gas hold-up in column flotation*, Inter. J. of Miner. Process. 157, 163-173. https://doi.org/10.1016/j.minpro.2016.10.005

VINNETT, L., URRIOLA, B., ORELLANA, F., GUAJARDO, C., ESTEBAN, A., 2022, *Reducing the presence of clusters in bubble size measurements for gas dispersion characterizations*, Minerals, 12, 1148. https://doi.org/10.3390/min12091148

VINNETT, L., YIANATOS, J., ALVAREZ, M., 2014, *Gas dispersion measurements in mechanical flotation cells: Industrial experience in Chilean concentrators*, Minerals Engineering, 57, 12-15. https://doi.org/10.1016/j.mineng.2013.12.006

Voigt, P., Hourn, M., Lawson, V., Anderson, G., Mallah, D., 2017. *Economic recovery and upgrade of metals from middling and tailing streams*. 49th Annual Canadian Mineral Processors Operators Conference, Ottawa, Ontario, 17-19 January.

WIBBERLEY, L., 2015. *Micronised refined carbons and the direct injection carbon engine*. John Sedgman Lecture, Brisbane Novotel, 10 June.

YIANATOS, J., BERGH, L., VINNETT, L., PANIRE, I., DÍAZ, F., 2015, Modelling of residence time distribution of liquid and solid in mechanical flotation cells, Minerals Engineering, 78, 69-73. https://doi.org/10.1016/j.mineng.2015.04.011

YIANATOS, J., CONTRERAS, F., DÍAZ, F., 2010, *GAS holdup and RTD measurement in an industrial flotation cell*, Minerals Engineering 23, 125–130. https://doi.org/10.1016/j.mineng.2009.11.003

YIANATOS, J., DIAZ, F., RODRIGUEZ, J., 2002, *Industrial flotation process modelling: rtd measurement by radioactive tracer technique*, IFAC Proceedings, 35(1), 55-60. https://doi.org/10.3182/20020721-6-ES-1901.01160

YIANATOS, J., VINNETT, L., PANIRE, I., ALVAREZ-SILVA, M., DIAZ, F., 2017, *Residence time distribution measurements and modelling in industrial flotation columns*, Minerals Engineering, 110, 139-144. https://doi.org/10.1016/j.mineng.2017.04.018

YIN, W., YANG, X., ZHOU, D., LI, Y., LÜ, Z., 2011. *Shear hydrophobic flocculation and flotation of ultrafine Anshan hematite using sodium oleate*. Transactions of Nonferrous Metals Society of China, 21(3), 652-664. https://doi.org/10.1016/S1003-6326(11)60762-0

YOU, X., LI, L., LIU, J., WU, L., HE, M., LYN, X., 2017, *Investigation of particle collection and flotation kinetics within the Jameson cell downcomer*, Powder Technology, 310, 221-227. https://doi.org/10.1016/j.powtec.2017.01.002

YOUNG, M.F., BARNES, K.E., ANDERSON, G.S., PEASE, J.D., 2006. *Jameson Cell: The "Comeback" in base metals applications using improved design and flow sheets*. 38th Annual Meeting of the Canadian Mineral Processors, Ottawa, Ontario, Canada, January 17–19, 311–332.

ZAHAB NAZOURI, A., SHOJAEI, V., KHOSHDAST, H., HASSANZADEH, A., 2021. *Hybrid CFD-experimental investigation into the effect of sparger orifice size on the metallurgical response of coal in a pilot-scale flotation column*, Inter. J. of Coal. Prepa. and Utiliz. https://doi.org/10.1080/19392699.2021.1960318